β-decay half-lives of neutron-rich N=82,81 isotones by shell-model calculations

Noritaka Shimizu[1,*], *Yutaka* Utsuno[2,1], and *Tomoaki* Togashi[1]

[1]Center for Nuclear Study, The University of Tokyo, Hongo, Bunkyo-ku, 113-0033 Tokyo, Japan
[2]Advanced Science Research Center, Japan Atomic Energy Agency, Tokai, Ibaraki 319-1195, Japan

Abstract. We perform large-scale shell-model calculations and successfully describe the low-lying spectra and half-lives of neutron-rich $N = 82$ and $N = 81$ isotones with $Z = 42 - 49$ in a unified way. Shell-model study shows that their Gamow-Teller strength distribution has a peak in the low-excitation energies, which significantly contributes to the half-lives. This peak is dominated by the $\nu 0g_{7/2} \rightarrow \pi 0g_{9/2}$ transition and enhanced on the proton deficient side of these isotones due to the Pauli blocking effect and the change of the effective single-particle energy of the $\nu 0g_{7/2}$ orbit.

1 Introduction

β-decay half-lives of neutron-rich nuclei around $N = 82$ are key data to understand the second peak of the solar abundance in the r-process nucleosynthesis [1]. The r-process path is considered to go through the neutron-rich region of the nuclear chart. Where the r-process path comes across the magic number $N = 82$, β decay and neutron capture occur alternately and form the waiting points of neutron captures in the r-process. After that, these nuclei cause multiple β-decays and reach the stability line of the nuclear chart, causing the second peak of the solar abundance. The half-lives of $N = 82$ and $N = 81$ isotones are important nuclear data for understanding the r-process nucleosynthesis. In the present work, we adopt nuclear shell-model calculations and investigate theoretically the β-decay properties of $N = 82$ and $N = 81$ isotones. This article is based on Ref. [2].

2 Shell-model calculations

We performed large-scale shell-model calculations to discuss β-decay properties of $N = 81$ and $N = 82$ isotones. The model space for the shell-model calculation is taken as $28 < Z < 82$ ($0f_{5/2}$, $1p_{3/2}$, $1p_{1/2}$, $0g_{9/2}$, $0g_{7/2}$, $1d_{5/2}$, $1d_{3/2}$, $2s_{1/2}$, and $0h_{11/2}$) for the proton orbits and $50 < N < 82$ ($0g_{7/2}$, $1d_{5/2}$, $1d_{3/2}$, $2s_{1/2}$, and $0h_{11/2}$) for the neutrons orbits with ^{78}Ni being an inert core. The shell-model interaction consists of the JUN45 interaction [3] for the f_5pg_9 space, the SNBG3 interaction for the neutron $50 < N < 82$ space [4], and the monopole-based universal interaction [5] for the rest part. We truncate the model space by restricting up to 2 proton holes in the pf shell and up to 3-particle 3-hole excitations across the $N = 50$ gap so that the calculation is feasible. Since the M-scheme dimension of the shell-model

*e-mail: shimizu@cns.s.u-tokyo.ac.jp

Hamiltonian matrix reaches 3.1×10^9 and is quite large, efficient usage of a supercomputer is essential. We employ the shell-model code KSHELL [6] for massively parallel computing. The Lawson method is applied to suppress the contamination of center-of-mass motion [7]. In Ref. [2], we demonstrated that the present shell-model interaction successfully reproduces the binding energies and low-lying spectra of $N = 80, 81$, and 82 nuclei, which confirms the validity of the present setup of the shell-model study.

3 Results and discussions

We employ the Lanczos strength function (LSF) method [8] to obtain the Gamow-Teller (GT) strength distribution. In this method, the initial state of the iterations is prepared as $O(GT)|\phi_p\rangle$, where $O(GT)$ is the Gamow-Teller operator, $\sigma\tau_-$, and $|\phi_p\rangle$ is the wave function of the parent nucleus. We performed 250 Lanczos iterations and evaluate the strength distribution in the subspace spanned by the Lanczos vectors. The quenching factor of the Gamow-Teller transition is taken as 0.7, which is widely used. We do not evaluate the first-forbidden transition since its contribution is expected to be rather unchanged [9] and can be absorbed into the quenching factor.

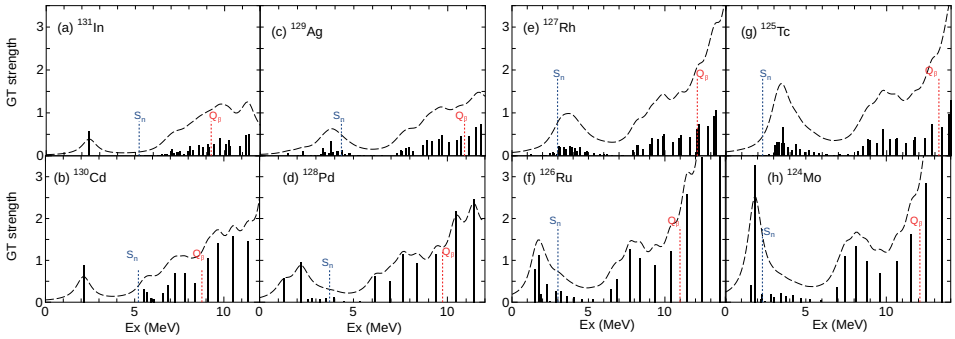

Figure 1. Gamow-Teller strength distribution of $N = 82$ isotones, (a) ^{131}In, (b) ^{130}Cd, (c) ^{129}Ag, (d) ^{128}Pd, (e) ^{127}Rh, (f) ^{126}Ru, (g) ^{125}Tc, and (h) ^{124}Mn, provided by the shell-model calculations. The blue and red dotted lines denote the neutron separation energies and Q-values, respectively. The dashed lines are the folded strength functions by a Lorentzian with 1-MeV width. Revised from Ref. [2].

Figure 1 shows the GT strength distribution of $N = 82$ isotones provided by the LSF method. While the strength of the low-energy peak of ^{131}In ($Z = 49$) at around $E_x = 2$ MeV is small, the strength grows gradually as the proton number decreases. In these isotones, the GT transition from the neutron $0g_{7/2}$ orbit to the proton $0g_{9/2}$ orbit is dominant for the β decay. At $Z = 50$, the proton $0g_{9/2}$ orbit is fully occupied and suppresses the Gamow-Teller transition because of the Pauli blocking. With decreasing the proton number from 50 to 40, the proton $0g_{9/2}$ orbit becomes vacant and the Pauli-blocking effect is weakened. Therefore, the GT strength is gradually enhanced as the proton number decreases till $Z = 40$. In addition, the evolution of the neutron $0g_{7/2}$ orbit contributes coherently to this enhancement as follows.

Figure 2 shows the neutron effective single-particle energies (ESPEs) of $N = 82$ isotones. The proton $0g_{9/2}$ orbit is fully occupied at $Z = 50$ and the ESPE of the neutron $0g_{7/2}$ orbit is the lowest among the five orbits, as indicated by the experimental energy levels of ^{131}Sn [10]. On the other hand, at $Z = 40$ the proton $0g_{9/2}$ orbit is vacant and the neutron $0g_{7/2}$ orbit is raised up and approaches the Fermi level because of the strong attractive monopole force

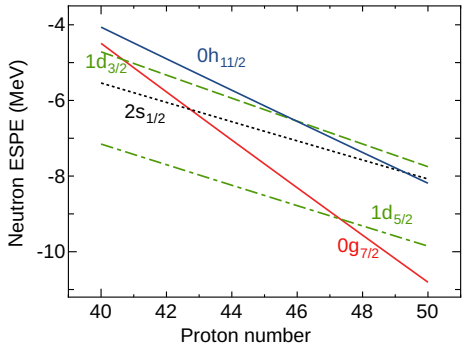

Figure 2. Neutron ESPEs of N=82 isotones. The blue solid, red solid, green dashed-dotted, green dashed, and black dotted lines denote the ESPEs of the neutron $0h_{11/2}, 0g_{7/2}, 1d_{5/2}, 1d_{3/2}$, and $2s_{1/2}$ orbits.

between the $\pi 0g_{9/2}$ and $\nu 0g_{7/2}$ orbits. This strong attractive force is caused by a cooperative attraction of the central and tensor forces [5].

The half-lives are evaluated by accumulating the transition probabilities from the parent ground state to the daughter states whose excitation energies are below the Q_β value. Figure 3 shows the beta-decay half lives of the $N = 81$ and $N = 82$ isotones. The present shell-model results shown as blue solid circles reproduce the experimental values quite well except that of ^{131}In. The half-lives provided by other theoretical models, such as preceding shell-model study [9], relativistic QRPA [11] and the gross theory with the KTUY mass formula [12, 13], are also shown in Fig. 3. These results show a certain overestimation, especially for $N = 81$ isotones.

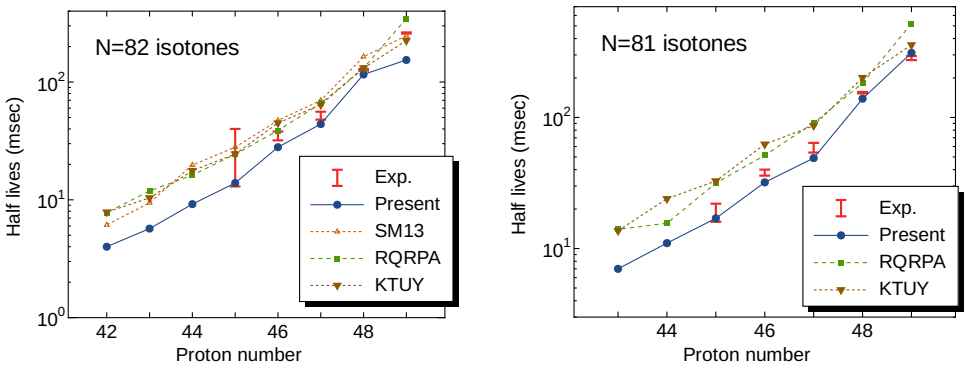

Figure 3. β-decay half-lives of $N = 82$ (left panel) and $N = 81$ (right panel) isotones. The red symbols with error bars denote the experimental values [14]. The blue circles, orange triangles, green squares, and brown inverted triangles denote those of the present shell-model study, the previous shell-model study [9], the relativistic QRPA [11], and the gross theory [13] with the KTUY mass formula [12], respectively.

4 Summary

We present shell-model results of the β-decay half-lives by the GT transition. The experimental half-lives of $N = 82$ and 81 isotones are well produced by the present shell-model study and some predictions are presented. The low-energy peak of the GT strength gradually increases as the proton number decreases from 50 to 40, which is caused by the Pauli-blocking effect of the proton $0g_{9/2}$ orbit and the ascension of the ESPE of the neutron $0g_{7/2}$ orbit coherently.

Acknowledgment

NS acknowledges Hiroyuki Koura for providing us with the KTUY results The authors acknowledge valuable supports by "Program for Promoting Researches on the Supercomputer Fugaku" (JPMXP1020200105), and "Priority Issue on post-K computer" (Elucidation of the Fundamental Laws and Evolution of the Universe) MEXT, Japan. A major part of shell-model calculations was performed on CX400 supercomputer of Nagoya University (hp160146) and Oakforest-PACS supercomputer (hp200130, hp170230, hp160146, xg18i035). We also acknowledge the KAKENHI grants (17K05433, 20K03981), JSPS, Japan.

References

[1] M. Mumpower, J. Cass, G. Passucci, R. Surman, and A. Aprahamian, AIP Advances **4**, 041009 (2014).
[2] N. Shimizu, T. Togashi and Y. Utsuno, Prog. Theor. Exp. Phys. **2021**, 033D01 (2021).
[3] M. Honma, T. Otsuka, T. Mizusaki, and M. Hjorth-Jensen, Phys. Rev. **C 80**, 064323 (2009).
[4] M. Honma *et al.*, RIKEN Accel. Prog. Rep. **45**, 35 (2012).
[5] T. Otsuka, T. Suzuki, M. Honma, *et al.*, Phys. Rev. Lett. **104**, 012501 (2010).
[6] N. Shimizu, T. Mizusaki, Y. Utsuno *et al.*, Comp. Phys. Comm. **244**, 372 (2019).
[7] H. Gloeckner and R. D. Lawson, Phys. Lett. **53B** 313 (1974).
[8] E. Caurier, G. Martinez-Pinedo, F. Nowacki, A. Poves, and A. P. Zuker, Rev. Mod. Phys. **77**, 427, (2005)
[9] Q. Zhi, E. Caurier, J. J. Cuenca-Garcia, K. Langanke, G. Martinez-Pinedo, and Sieja, Phys. Rev. C **87**, 025803 (2013).
[10] NuDat 2.8, http://www.nndc.bnl.gov/nudat2/.
[11] T. Martekin, L. Huther, and G. M.-Pinedo, Phys. Rev. C **93**, 025805 (2016).
[12] H. Koura, T. Tachibana, M. Uno, and M. Yamada, Prog. Theor. Phys. 113 (2005) 305.
[13] T. Tachibana and M. Yamada, Proc. Inc. Conf. on exotic nuclei and atomic masses, Arles, 1995, eds. M. de Saint Simon and O. Sorlin (Editions Frontueres, Gif-sur-Yvette, 1995) p.763. and references therein; T. Yoshida and T. Tachibana, Journal of Nuclear Science and Technology, **37** 491 (2000); T. Tachibana, RIKEN Review, Focused on Models and Theories of the Nuclear Mass, **26** 109 (2000).
[14] G. Lorusso, S. Nishimura, Z. Y. Xu *et al.*, Phys. Rev. Lett. **114**, 192501 (2015).